Development of New Thermal Protection Systems Based on Polysiloxane/Silica Composites

Kurt J. Schellhase[1], Ethan Liu[2], Ty Templin[3], Noel Arguello[4], Logan Head[5], Andrew Adlof[6], and Joseph H. Koo[7]
The University of Texas at Austin, Austin, TX 78712, USA

Jarrod J. Buffy[8]
Dyna-Glas Technologies LLC, Perrysburg, OH, 43551, USA

James Cerda[9]
Texas State University, San Marcos, TX, 78666, USA

Nomenclature

TPS	=	Thermal Protection System
SOTA	=	State of the Art
TGA	=	Thermogravimetric Analysis
MCC	=	Microscale Combustion Calorimeter
HRC	=	Heat Release Capacity
HRR	=	Heat Release Rate
FRP	=	Fiber Reinforced Polymer
BMC	=	Bulk Molding Compound
OTB	=	Oxy-acetylene Test Bed
DG	=	Dyna-Glas
S/DG	=	Silica/Dyna-Glas

I. Introduction

Ablative materials are widely used in the aerospace and defense industry. This class of material has unique properties, which allows them to resist the high heat flux environment experienced by spacecraft and rocket motors. Some of the most advanced thermal protection systems, vertical launching systems, and rocket motors contain ablative composites utilizing fiber reinforced SC-1008 phenolic ablative systems.

While many ablatives in use today consist of SOTA resins, such as phenolic and cyanate ester, there is a need for new ablative materials, which can withstand higher temperatures and heat fluxes. Better ablatives allow for weight-savings and better performance for advanced propulsion systems and thermal protection systems for reentry vehicles. One such application is atmospheric entry probes, which can encounter very harsh reentry environments due to high speeds experienced during planetary entry, such as the Galileo probe sent to Jupiter. It utilized thick carbon/phenolic TPS.[1,2] A report by NASA Ames after the mission determined that future missions to the planet, especially ones utilizing multiple probes, would require a "new, robust, and efficient TPS."[2] The most recent development in ablative TPS materials by NASA has been 3D woven cyanate ester composites that act as both a compression pad and ablative

[1] Student, Mechanical Engineering Dept., 1 University Station C2200, Austin, TX 78712
[2] Student, Mechanical Engineering Dept., 1 University Station C2200, Austin, TX 78712
[3] Student, Mechanical Engineering Dept., 1 University Station C2200, Austin, TX 78712
[4] Student, Mechanical Engineering Dept., 1 University Station C2200, Austin, TX 78712
[5] Student, Mechanical Engineering Dept., 1 University Station C2200, Austin, TX 78712
[6] Student, Mechanical Engineering Dept., 1 University Station C2200, Austin, TX 78712
[7] Senior Research Scientist and Director, Polymer Nanocomposites Technology Lab, Department of Mechanical Engineering, 204 E. Dean Keeton St./C2200, Austin, TX 78712-0292; AIAA Associate Fellow; *Corresponding author: jkoo@mail.utexas.edu
[8] CTO, Dyna-Glas Technologies LLC, 2100 N. Wilkinson Way Perrysburg, OH 43551
[9] Student, Texas State Advanced Composites Lab, 601 University Dr, San Marcos
San Marcos, TX 78666

heat shield for the new Orion spacecraft.[3] Stronger TPS ablatives can also minimize the amount of material needed to protect the primary structure of the rocket and involve less weight to the overall structure of the vehicle.[2] One resin system that is showing strong potential as a new TPS material is the DG-UHTR polysiloxane based resin system.

We have been investigating material properties of three neat resins: SC-1008 phenolic, PT-15 cyanate ester, and DG-UHTR polysiloxane. Experiments were carried out to compare the char yield, thermal stability, flammability, and kinetic parameters of each neat resin. By analyzing the char yield of each material, it allows us to focus on an important part of the TPS's function, the creation of a protective char layer as it undergoes pyrolysis. As surface of the TPS begins to thermally degrade and form a porous char layer, it acts as a sacrificial layer, providing an extra layer of thermal insulation to the TPS until higher temperatures allow it to undergo oxidization or be removed by external forces from the hypersonic gas flow.[4,5] This char blocks heat and oxygen from reaching the virgin TPS material, while regulating the release of the cooling pyrolysis gases.[4] This study focuses on the development and characterization of new ablative materials that can be equal or exceed legacy materials utilizing SOTA resins.

II. Neat Resin Systems

SC-1008 is MIL-standard phenolic resole resin manufactured by Hexion.[6] It is the most commonly used resin for manufacturing ablative, such as carbon/phenolic (Cytec's MX4926N used for solid rocket motor nozzle), silica/phenolic (Cytec's MX2600 used for solid and liquid rocket motor nozzles), and in PICA. This phenolic resole resin has a char yield of 56%.

PT-15 is a low viscosity cyanate ester (CE) resin manufactured by Lonza.[7] It is a common resin used for high-temperature application. This CE is very similar to the Tencate EX-1510 CE resin used by Feldman *et al.* 3D woven multifunctional ablative TPS for Orion.[3,8] This cyanate ester resin has a char yield of 57%.

DG-UHTR resin is formulated using a proprietary (patent pending), inorganic matrix of a variety of polysiloxane chemistries. It is a resin system tailored to produce TPS laminates.[9] Dyna-Glas Technologies, LLC is the manufacturer and recently introduced a series of ceramic matrices specifically designed as binders for composite materials as flame shielding barriers. This system offers the uniqueness of a low temperature cure resin system that exhibits an extreme resistance to a high temperature environment. It also possesses properties, such as low thermal transfer, excellent chemical resistance, low to no smoke or toxic fumes when exposed to flame sources. These are fire, smoke, and toxicity (FST) characteristics that are desirable for fire resistant polymers. The DG-UHTR resin system in this study was found to have a char yield of 87%.

III. Characterization of the Neat Resin Systems

To better understand the thermal properties of the polysiloxane based resin system, a cured coupon of the neat DG-UHTR resin system was characterized. The SC-1008 phenolic and PT-15 cyanate ester resins were also prepared, in order to compare the new system to the current SOTA resins. We chose to focus in on the thermal properties of each resin using TGA and MCC. We are also in the process of determining activation energy using computer modeling. In order to better understand the ablation behavior of each resin system, we first wanted to define a standardized method of finding a materials char yield. In a recent char yield study conducted by Koo *et al.*,[10] conditions were developed for char yield determination with standard test procedures based on the NASA PICA report.[11]

The char yield was measured using a TA Instruments Hi-Res TGA 2950 Thermogravimetric Analyzer with a material sample size of 20 mg. The samples were dried using an isothermal (constant temperature) at 150ºC (325ºF) for 30 minutes in nitrogen. Then a heating rate of 20ºC/min from 150ºC to 1,000ºC in nitrogen was applied. The initial weight (100% weight) was taken after the 30 minute drying. The char yield is defined as the weight % at 1,000ºC.

Table 1. Char yield and 10% mass loss data for the three resin systems.

	10% Mass Loss Temperature (°C)				Weight % at 1000°C			
	5°C / min.	10°C / min.	20°C / min.	40°C / min.	5°C / min.	10°C / min.	20°C / min.	40°C / min.
SC-1008	416	439	473	557	61.38%	57.54%	56.21%	56.99%
PT-15	474	491	514	550	60.61%	57.69%	56.85%	55.44%
DG-UHTR	690	704	765	990	85.85%	85.87%	86.48%	90.20%

The char yield studies were performed on neat resin samples of SC-1008, PT-15, and DG-UHTR. Figure 1 shows the TGA curves of each resin and table 1 shows the decomposition temperature (T_d) at 10% mass loss and the char yield at 1,000ºC. As seen in figure 1, the resins gave the following char yeilds: SC-1008 = 56.21%, PT-15 = 56.85%, DG-UHTR = 86.48%. Figure 2 shows the derivative of the TGA data, dTGA (%/ºC), for the three neat resins. The temperature of the peaks of the dTGA, T_d at 10% mass loss, and % weight at 1,000ºC are noted on the graphs.

From the Figure 2, the dTGA of SC-1008 shows three distinct reactions occur at 410, 497, and 655ºC, this resin system exhibits 3 transitions that are reported for phenolic resins.[14] PT-15 shows only one reaction occurs at 511ºC, suggesting a uniform decomposition for this resin system. DG-UHTR shows two distinct reactions occur at 722 ºC and 873ºC. The DG-UHTR resin also has the highest T_d at 10% mass loss (765ºC) amongst the resin systems. Thus, the DG-UHTR resin appeared to be a viable candidate for FRP ablatives.

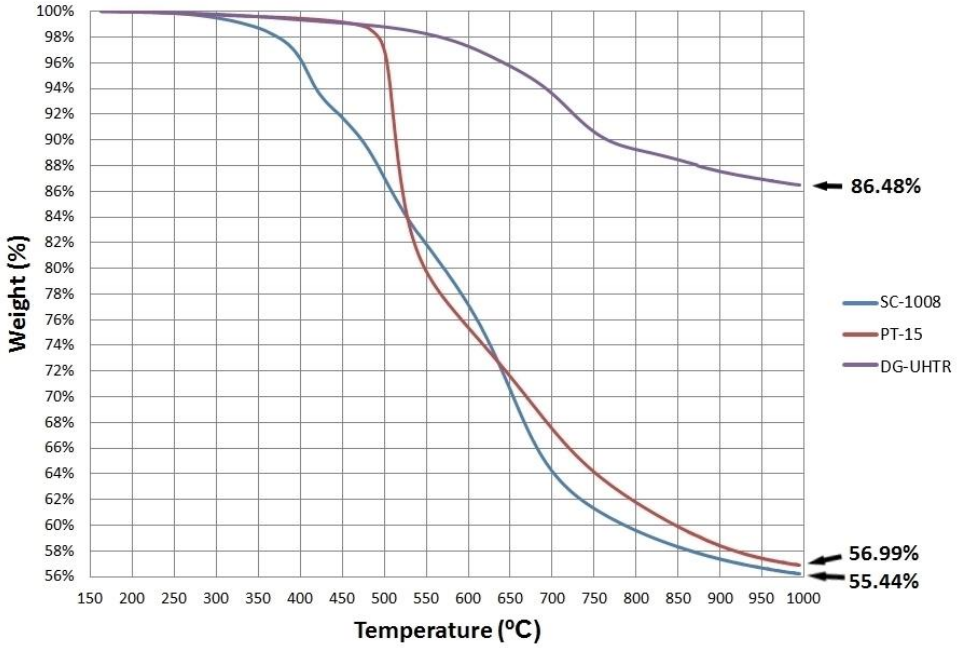

Figure 1. Char yield results for SC-1008, PT-15, and DG-UHTR.

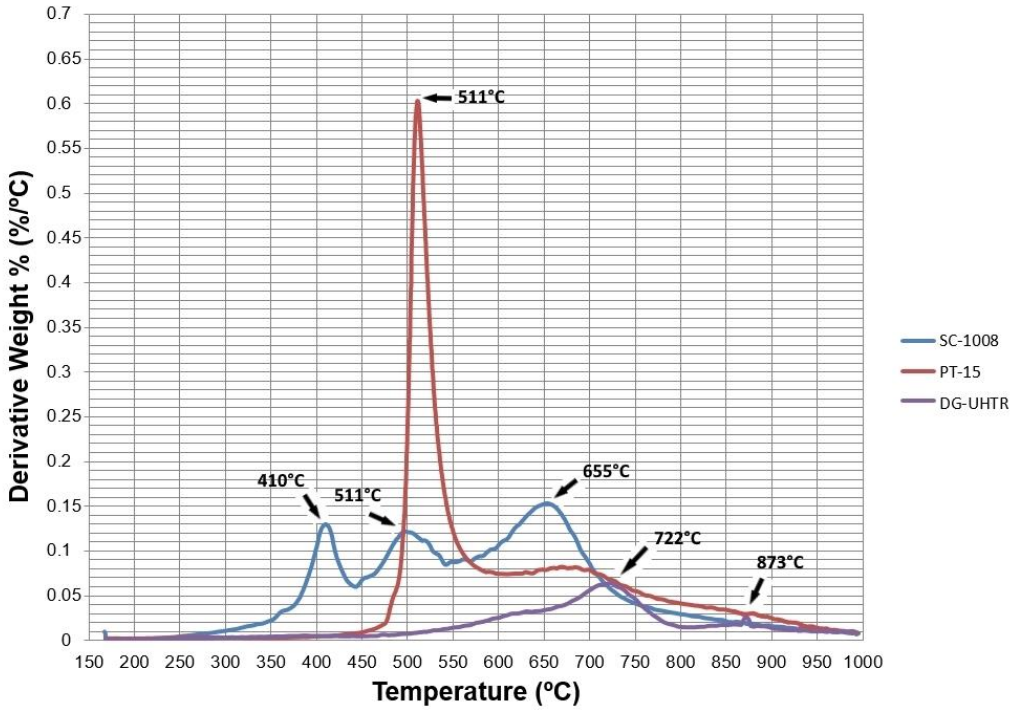

Figure 2. dTGA (%/ºC) data for SC-1008, PT-15, and DG-UHTR

.

Flammability properties were determined by MCC tests. MCC, developed by FAA, measures the heat release rate of milligram sized samples. It's a convenient tool to screen material's flammability properties and a cheaper tool than cone calorimetry.[12]

The typical MCC heat release curves of the three resins are plotted in Figure 3. The DG-UHTR showed a peak HRR at around 630°C. The DG-UHTR resin also showed a peak at 750°C, there may be another heat release peak above 750°C. More investigation in the future is needed to confirm this observation. PT15 has one major HRR peak at 455.9°C. The peak HRR of PT15 is significantly higher than the other two resins indicating its relatively poor flame resistant properties. SC1008 have three distinct HR peaks, the overall HRR values are also higher than that of the DG-UHTR.

Calculated from MCC data, heat release capacity (HRC) is an intrinsic material property independent of heating rate and.[14] The HRC comparison of the three

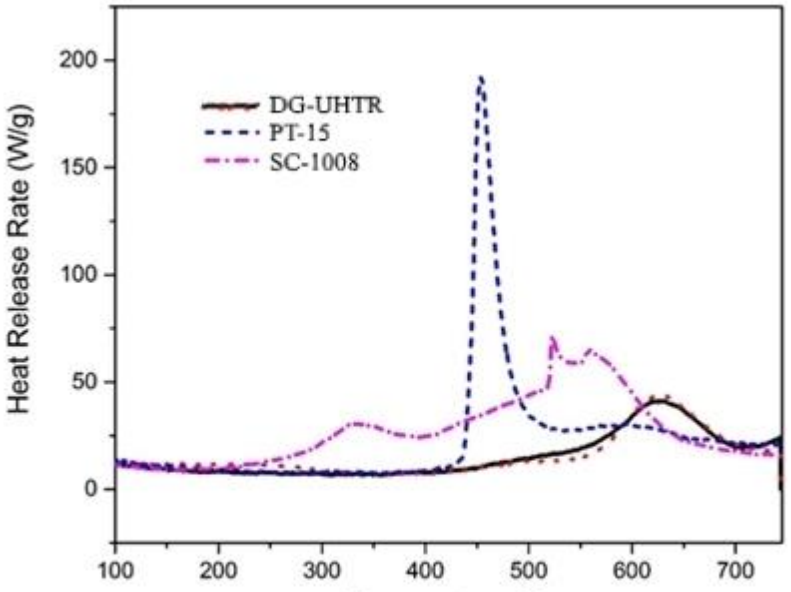

Figure 3. Typical Heat Release Curves for the three resin systems.

resin systems are shown in Figure 9. DG-UHTR showed a HRC of 36 J/g-K. On the other hand, because of the high PHRR of PT15, a much higher HRC of 159.3J/g-K is not surprising. SC1008 has HRC of 53.3J/g-K which is 48% higher HRC than that of the DG-UHTR.

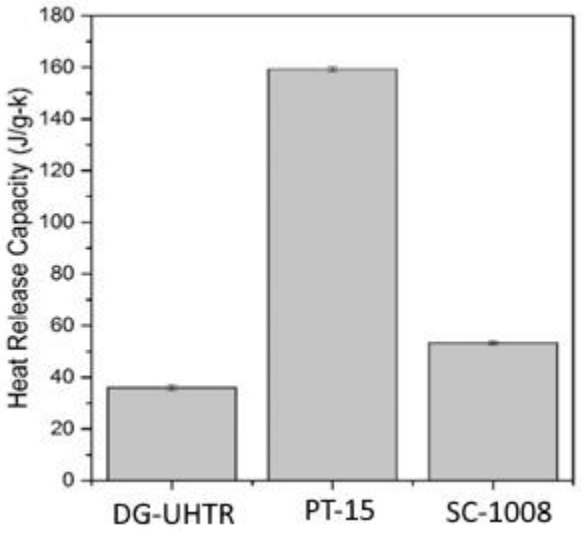

Figure 4. Comparison of the Heat Release Capacities for the three resin systems

IV. Composite Materials

To fully evaluate the DG-UHTR resin's effectiveness as an ablative material, we needed to create a FRP. We decided to compare the effectiveness of silica/DG-UHTR against silica/phenolic. Silica/phenolic is a commonly used in industrial and aerospace applications, with one of the premier materials being Cytec's MX-2600, which was used as the control for our study. This ablative utilizes the MIL-R-9299, Type II phenolic resin (64wt%), silica fabric(30-35wt%), and silica powder (4.5wt%).[16]

The DG-UHTR polysiloxane resin was generously provided by Dyna-GlasGlas LLC., and contained 35wt% IPA as the solvent. Aerospace grade 99% SiO_2 content silica fabric was purchased from Cytec, with nominal weight of 19 oz/yd^2. The silica fabric was impregnated with DG-UHTR resin using the hand-layup method, it was observed that the polysiloxane resin easily infiltrated the silica fabric and showed good wettability. The wetted fiber was subsequently heated under -5psi vacuum at 120°C for 5hr to remove all of the IPA. The prepreg laminates were then removed from the oven and chopped into ½" by ½" squares, which were then used for compression molding the final composites. A cylindrical mold preheated to 170C was utilized in order to press the BMC. The BMC was first held at 170°C for 30min and 100PSI, then the temperature was increased to 100PSI and 260C for 120min. The mold was then allowed to cool to room temperature under pressure. A 75mm diameter by 16mm thick cylinder was produced from the mold, which was then waterjet into 15.5mm by 16mm thick cylindrical test samples. Two different S/DG-UHTR samples were made: F2 and F3, which contained 40wt% and 48wt% resin content. The densities of these two composites were measure using the water displacement method descried by ASTM D792-13 and it was found that F2 was 1.66g/cc and F3 was 1.62g/cc. Each lower than the MX2600's 1.71g/cc, likely due to containing less silica fabric.

V. Characterization of the Ablative Composites

A. Experimental Setup

An OTB, as seen in figure 5, was used to simulate re-entry conditions and evaluate the DG-UHTR's potential as an ablative material. The Oxy-acetylene torch utilized a Viktor #W-4 torch tip, and was supplied by 12.2 SLPM oxygen and 9 SLPM acetylene to yield a 1.35 Oxygen:Fuel ratio. A gardon gauge (Medtherm) was used to locate the distance from the torch needed to achieve a 1000 W/cm^2 flame, 19.8mm. Each sample was exposed to the flame for 40 seconds.

The cylindrical test samples had a hole drilled in the back face to insert a 0.55mm diameter K-type thermocouple such that it was 10mm from the samples testing face. This was used to measure the peak heat soak temperature within the material, a useful metric for comparing insulative materials. A carbon-carbon shield and silica insulation was used to protect the backside thermocouple from flame warp around during testing.

An infrared and high-definition camera were utilized during testing to gain insight on how the material behaves while in contact with the torch. A two-color infrared pyrometer, which measures temperature independent of emissivity, was utilized to monitor the surface temperature of the samples.

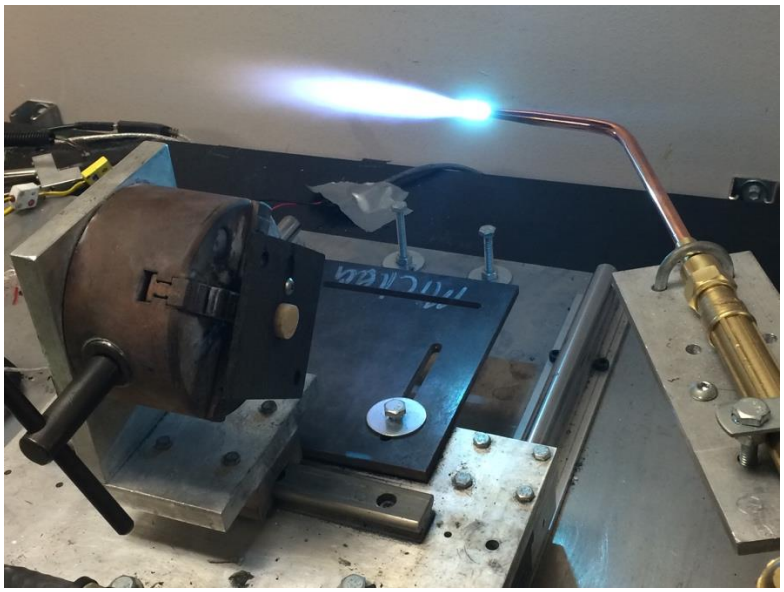

Figure 5. The OTB testing setup

Figure 6 shows a S/DG-UHTR and MX2600 samples before and after being exposed to the OTB. The 40 seconds of exposure charred a majority of each sample. Upon visual inspection, the post-test F2 and F3 samples look nearly identical, however, the char of the F3 samples was more fragile, and could be broken off easily. The F2 and MX2600 samples were easy to handle post-test and were quite rigid. The DG-UHTR samples were composed of a black char with a blue/silver tint, with small beads of more reflective colors throughout the surface. The post-test MX2600 also showed this same color pattern, but the center of the ablative had a solid metallic gray color to it.

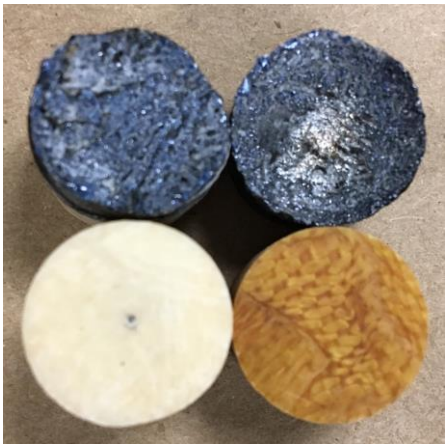

Figure 6. A S/DG-UHTR F2 Sample pre-test (bottom left) post-test (top left) and a MX2600 Sample pre-test (bottom right) post-test (top right)

B. Heat Soak, Recession Rate, Mass loss, and Surface Temperature Data

After testing each sample, the backside temperatures provided by the thermocouple were plotted against time as shown in figures 7,9, and 11. This value provides insight into how well the materials are performing as insulators. The maximum temperature recorded, also known as the peak heat soak temperature is a phenomenon that occurs because the ablative materials are excellent insulators, so instead of immediately dissipating absorbed heat like a metal might, the heat continues to travel through the sample increasing the internal temperature. This heat soak temperature occurs after the sample has been removed from the test flame. The time taken to reach this temperature is another important value which indicates how effective the sample is at insulating heat. The recession rate of the material proved to be very consistent at 0.058 mm/s, the char appeared tough and easy to handle.

As shown in figure 7 and table 2, the peak heat soak temperatures for the control samples averaged at 388.2°C. The surface temperature for every MX2600 sample measured consistently around 2050°C for the entire duration of the test, as seen in figure 8.

Table 2. Ablation testing data

	Density (g/cc)	Heat Soak Temperature (°C)*	Heat Soak Time (s)*	Recession Rate (mm/s)	Mass Loss (%)	Mass Loss Rate (g/s)
S/DG-UHTR F2	1.66	317.5 ± 3.5	102.2 ± 4.15	$0.054 \pm 4x10^{-3}$	$19.5 \pm 5x10^{-1}$	$0.022 \pm 1x10^{-4}$
S/DG-UHTR F3	1.62	318.17 ± 20.3	99.37± 6	$0.047 \pm 7x10^{-3}$	$19.3 \pm 6x10^{-1}$	$0.023 \pm 6x10^{-4}$
S/Ph MX2600	1.71	388.2 ± 18	88.93 ± 2.7	$0.058 \pm 2x10^{-3}$	$31.0 \pm 7x10^{-1}$	$0.031 \pm 3x10^{-4}$

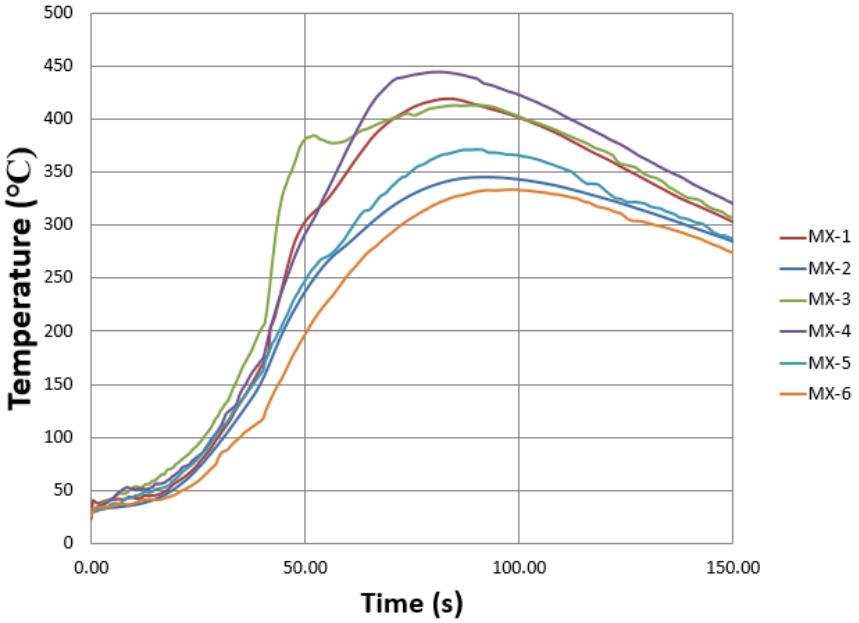

Figure 7. MX2600 Backside Temperatures

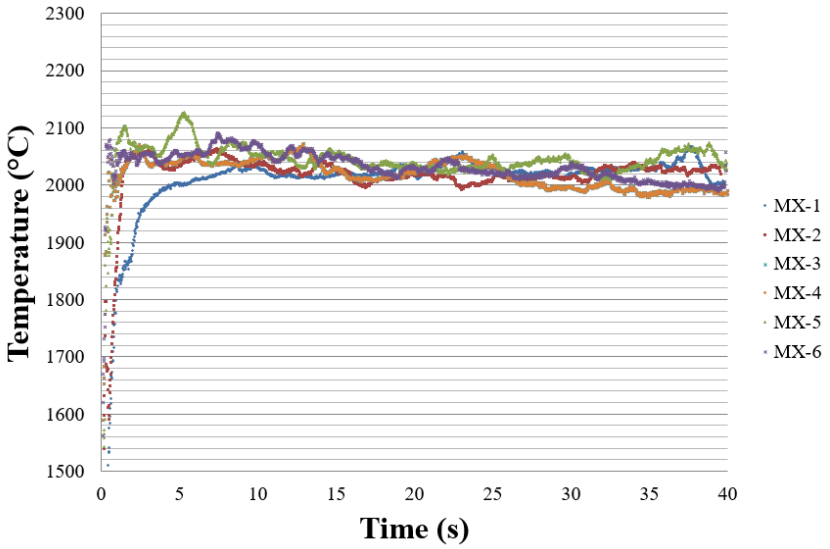

Figure 8. MX2600 Surface Temperatures.

The F2 samples, containing a 40%wt resin content, were tested next. The average backside temperatures experienced by this formulation were lower than the control by 18%. The F2 S/DG-UHTR composite showed a slightly slower recession rate as well. The heat soak temperature for these samples, as seen in Figure 10, was consistently low, with an average peak heat soak temperature of 317.5°C, which was 19% lower than the MX2600. The mass loss rate and percent were the biggest improvement from the control, with the F2 sample showing a 37% lower mass loss rate and 30% lower mass loss percent. The recession rate was very similar to MX2600, only slightly lower than the control at 0.054mm/s, which is within error. The char was tougher than the F3 sample and was easy to handle by hand.

The surface temperatures of the samples containing DG-UHTR resin were found to vary much more than the control. This may be since the DG-UHTR/silica composites tested are pre-ceramic materials which, form a ceramic while ablating. Since this occurs, the surface temperature may be affected because this is where the largest temperature is. Many of the tests spent time below the MX's average 2050°C, but would fluctuate during testing. The uneven surface of the ablating sample as seen later in the IR and HD camera images helps explain the range of temperatures seen on the samples surface.

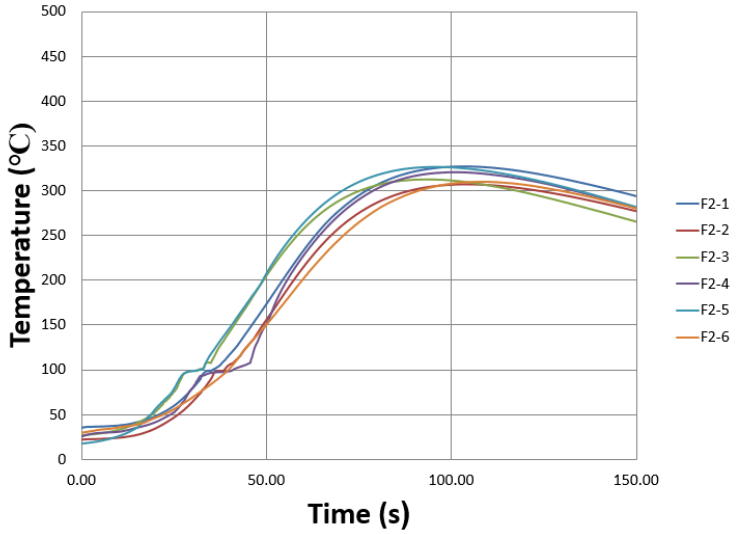

Figure 10. F2 Backside Temperatures.

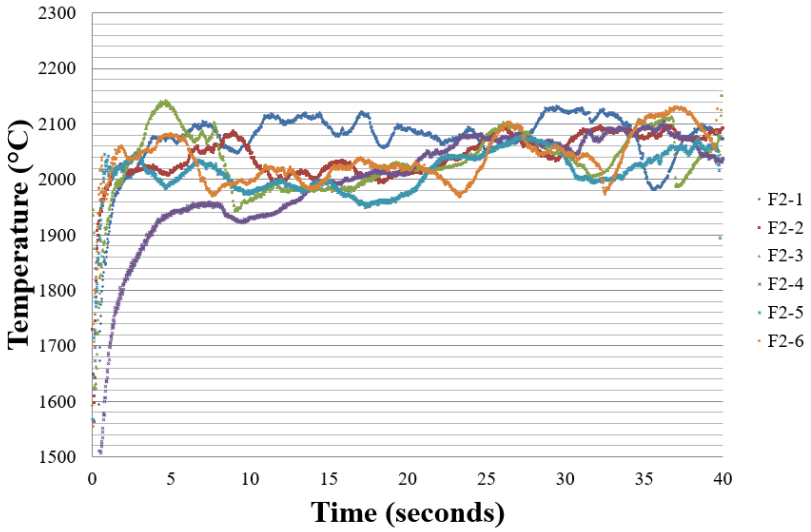

Figure 11. F2 Surface Temperatures.

Finally, the F3samples showed similar results to the F2 samples. As shown in figure 12, the heat soak temperatures were widely varied between 271°C and 411°C. With more samples tested, all but one sample had a peak heat soak temperature below 325°C each value was less than the previously tested formulations. With an average heat soak temperature of 318.17°C, it's within the margin of error of the F2's heat soak temperature and heat soak time. However, the, F2 sample was much more consistent, with lower margins of error. As seen in table 2, the F3 sample showed nearly identical mass loss rates and mass loss percent to the F2 sample. This formulation showed the lowest recession rate at 0.047mm/s, however, it was observed that this material swelled more than the others, giving way to a more delicate char that was not as sturdy and easy to handle.

As seen in figure 13, the surface temperature varied heavily compared to the F2 and MX2600 samples. The f3 samples had a larger variation in the surface temperature compared to F2. More of the F3 samples spent time above the 2050°C than the F2 samples.

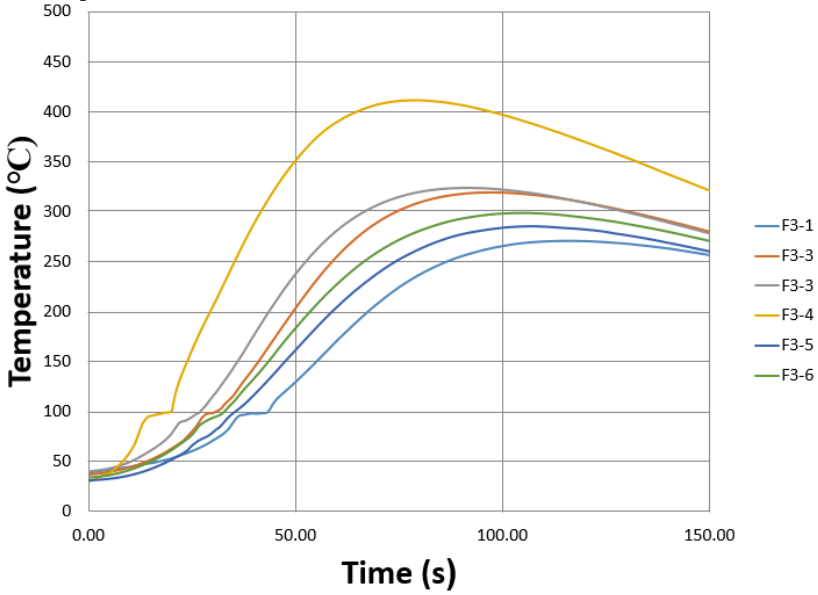

Figure 12. F3 Backside Temperatures.

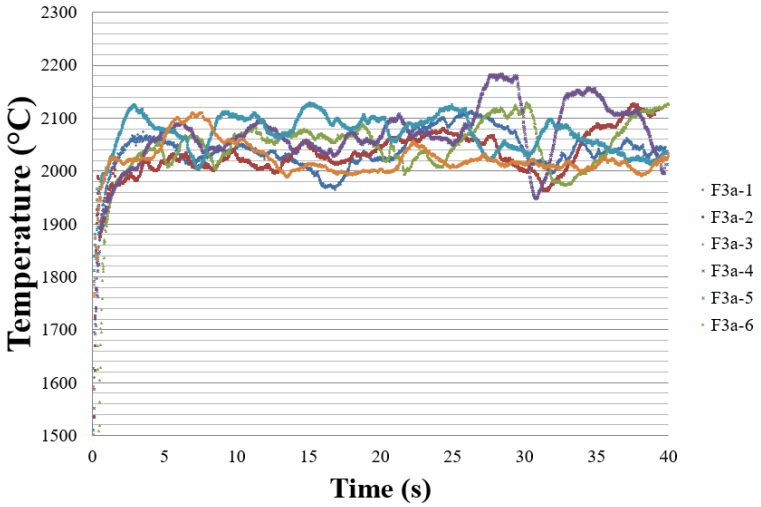

Figure 13. F3a Surface Temperatures.

Since the max heat soak temperature isn't reached until well after the torch has been removed, it is important to compare how long it takes to reach this maximum as well as what the max temperature is so that the sample's thermal absorption abilities can be better compared for reentry vehicle application. As seen in Table 2, the heat soak values for DG-UHTR are promising. Most of the F2 and F3 samples provided a much lower heat soak temperature than the MX control samples. The F2 samples provided a best backside temperature readings. The F3 samples provided an even better backside temperature reading a greater uncertainty of ± 20.3. This greater uncertainty is mostly due to a major outlier temperature reading of 411 °C, with the rest of the readings averaging to be about 300 °C. Both these F2 and F3 samples had much better heat soak temperatures than the MX control sample, which held an average heat soak of 388 °C and uncertainty of ±18.

C. IR Camera Images

Using the IR camera, heat map videos of the F2 and F3, and the MX2600 were made. The heat maps are a useful tool in displaying a broad visual representation of the surface temperature data along the whole front face of each sample, since the IR pyrometer can only focus on a single point. Figure 14 displays heat maps from the three tested materials at different periods during the 40s test. All three materials displayed a relatively uniform temperature distribution along its face. When comparing the heat maps of samples F2 and F3 with their respective palette bars, the data suggest both samples have an average surface temperature between 1900 and 2000 °C.

Unlike the S/DG-UHTR composites, the MX2600 sample displayed on the 10s image still from the MX test, has an orange hot spot on the left side of its front surface indicating a hotter region. This hotter region during the first 10s of the test was constantly seen on all MX samples. The cameras software was used to measure this region, showing a temperature spike of 2250 °C. These hotter regions will cause the MX2600 degrade quicker in those regions, resulting in quicker failure of the ablatives protection mechanism. It's possible that the DG-UHTR's ability to avoid surface temperature spikes and maintain a relatively constant surface temperature is advantageous for an ablative. However, at the same time, the DG-UHTR shows higher variability in the surface temperature later in the test than the MX does. Resulting the in the higher variability in surface temperature seen using the IR pyrometer focusing on one spot. You can see the mixture of dark and light green regions on the F2 and F3 samples, were the MX sample is more of a uniform color.

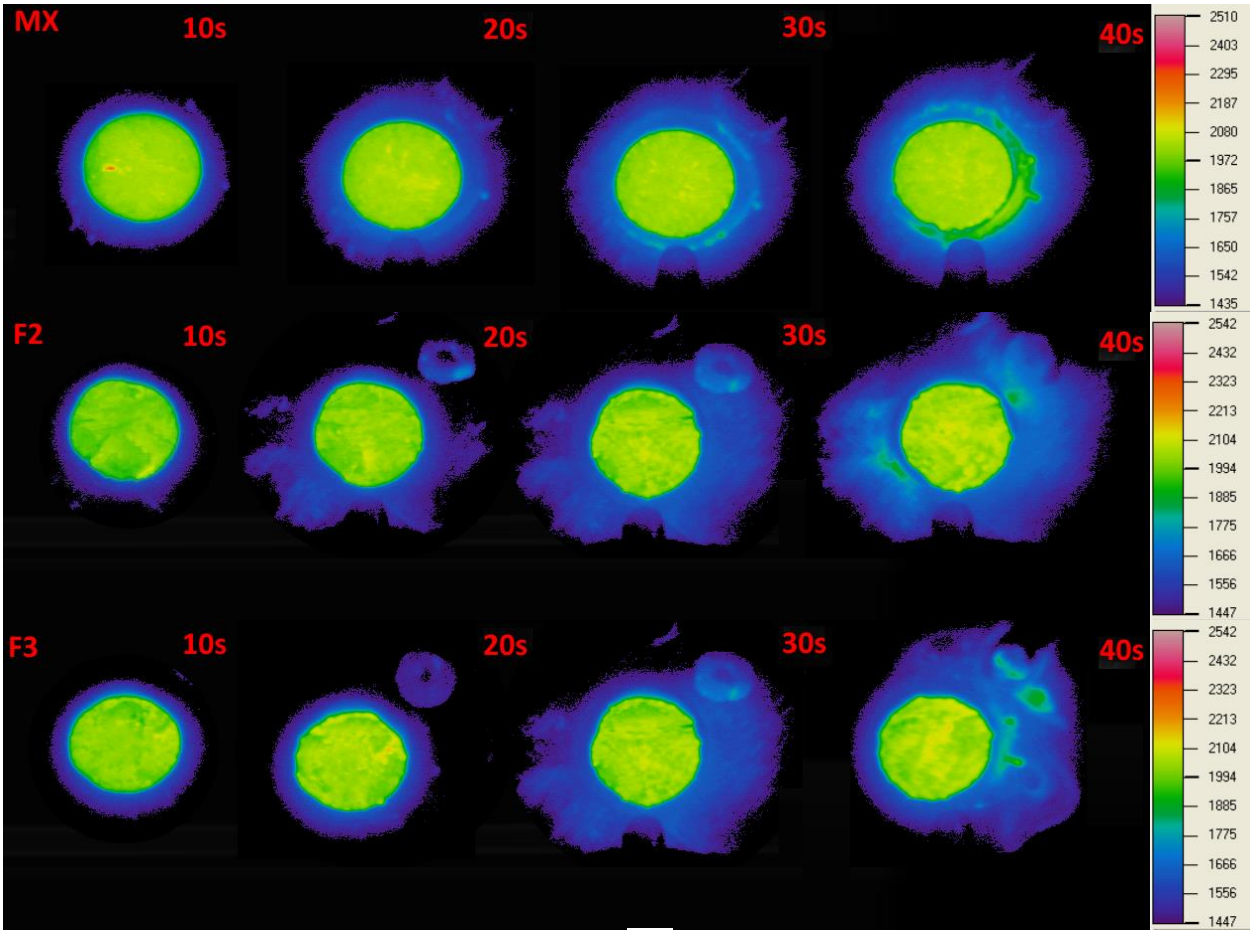

Figure 14. IR Camera Surface Temperature (° C) Heat Map at 20 Seconds of Exposure; Left: F2; Center: F3a; Right: MX2600.

D. HD Camera Images

Seen below in figure 15 are the HD camera stills from the same samples shown in figure 14. Both the S/DG-UHTR samples showed more flow from liquid-like materials on the surface towards the outer edges, presumably molten silica. It appears easier to make out the individual silica fabric squares as the resin degrades. The F3 and F2 had few differences, with the F3 showing a slightly more uneven surface during testing. As also seen in the IR footage, this results in jagged surfaces which results in regions of slighter cooler temperatures, as seen in the darker regions of the samples. This movement of surface material also accounts for the variability in the IR pyrometer surface temperature measurements, as they can only fix on one point of the changing surface.

Comparatively, the MX samples had a more evenly distributed surface texture. The footage showed some spherical aggregates on the MX samples as well, likely the melted silica fabric and filler, moving around on the surface. You can also see the brighter region on the 10s mark of the MX sample, where a bright light can be seen were the IR camera saw the hot spots which occurred during MX tests.

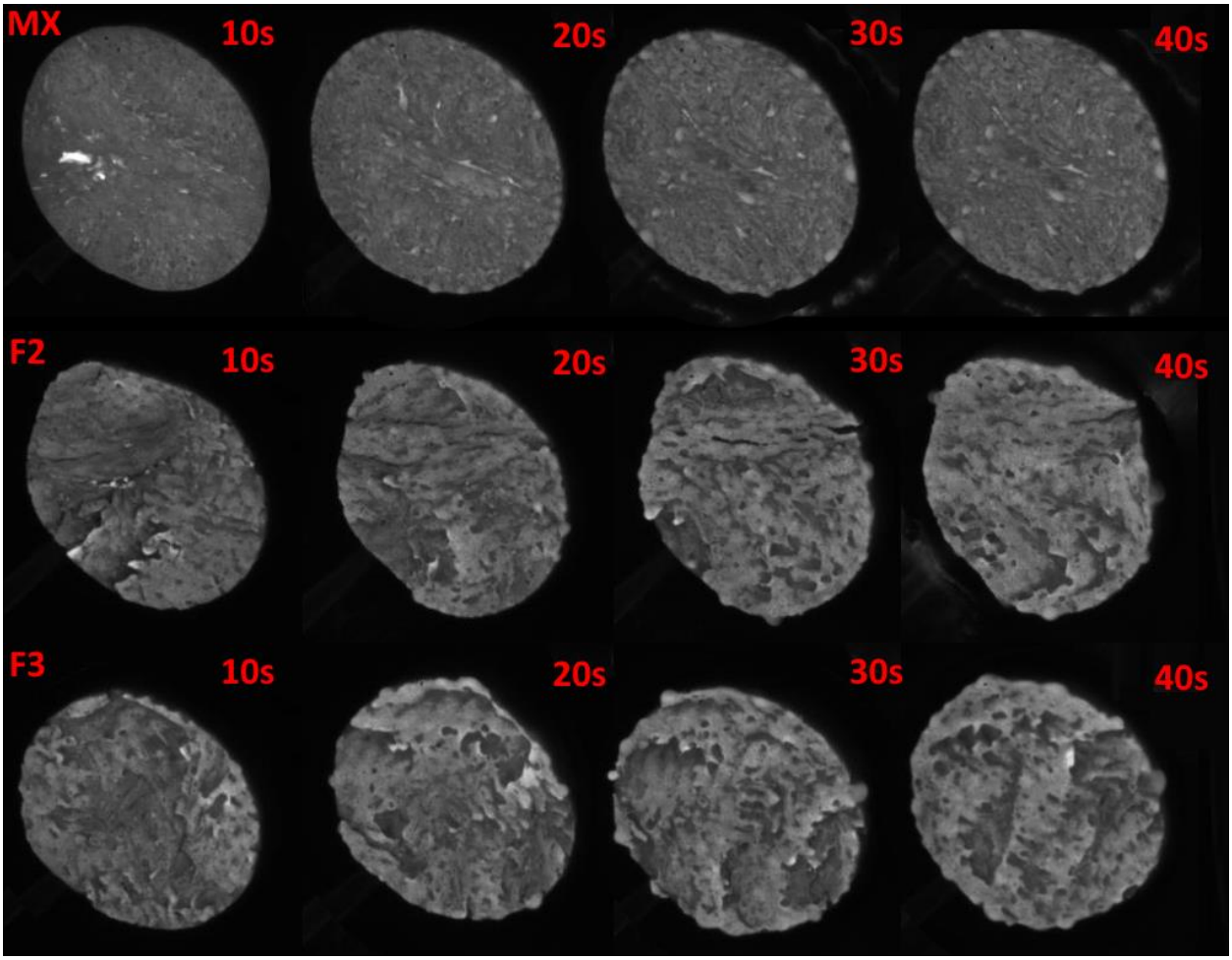

Figure 15. HD Camera Images of Sample MX2600; Left to Right: 10, 20, 30, and 40 Second Exposure Time.

VI. Conclusion

Our research on the silica polysiloxane composite has proven promising, showing distinct improvements from the industry standard phenolic. The greatest improvement seen was an average 19% and 9% slower recession rate for the the F3 (48%) and F2(40%) samples when compared to the MX2600 samples. Along with this, the DG-UHTR materials showed good insulative properties. The heat soak temperatures showed that the F2 and F3 formulations both had 18% lower peak heat soak temperatures. The thermal wave was also shown to move slower through the F2 and F3, with samples showing a 14.9% and 11.7% longer times to reach the peak heat soak temperature. showing that the insulating properties were greater among F2 and F3. The F2 S/DG-UHTR material also showed roughly 37% lower mass loss rate and 30% lower mass, owing to its high char yield. The density was also lower so that excessive weight when compared to the phenolic should not be an issue. The demand for a ablatives other than phenolic is pushing ablative research to search for new high performing materials. While outlook on the research we have completed for the S/DG-UHTR looks promising.

References

[1] B. Laub, E. Venkatapathy, E., "Thermal Protection System Technology and Facility Needs for Demanding Future Planetary Missions." *International Workshop on Planetary Probe Atmospheric Entry and Descent Trajectory Analysis and Science*. Lisbon, Portugal, 6-9 Oct. 2003, Retrieved 5-31-2015.

[2] F. S. Milos, "Galileo Probe Heat Shield Ablation Experiment," *Journal of Spacecraft and Rockets*, 34 (6), (1997): 705-713.

[3] J. Feldman *et al.*, "Development of a 3D Multifunctional Ablative Thermal Protection Systems for Orion," *National Space & Missile Materials Symposium*, Chantilly, VA, June 22-25, 2015.

[4] L. Torre, J. M. Kenny, and A. M. Maffezzoli, "Degradation behaviour of a composite material for thermal protection systems Part I – Experimental characterization," *Journal of Materials Science*, 33 (12), (1998): 3137-3143

[5] R. A. Vaia *et al.*, "Polymer/layered silicate nanocomposites as high performance ablative materials," *Applied Clay Science*, 15(1), (1999): 67-92.

[6] Hexion technical datasheet of SC-1008 phenolic resole resin.

[7] Lonza technical datasheet of PT-15 cyanate ester resin.

[8] J. Feldman *et al.*, "Development of an Ablative Quartz/Cyanate Ester Composite for the Orion Spacecraft Compression Pad," *Proc. CAMX 2015*, Dallas, Oct 24-28, 2015.

[9] Dyna-Glas technical datasheet, Kansas City, MO, accessed Jan 2016.

[10] J. Koo *et al.*, "Char Yield Studies of Several High-Temperature Resin Systems for Ablative Thermal Protection Systems," unpublished data, Feb. 2016.

[11] "PICA Material Property Report C-TPSA-A-DOC-158" for Crew Exploration Vehicle Block II Heatshield Advanced Development Project, NASA Report, Rev. 1, June 8, 2009, ITAR report received from NASA-Johnson Space Center, Houston, TX.

[12] R. E. Lyon, R. Walters. *A Microscale Combustion Calorimeter*. DOT/FAA/AR-01/117, Office of Aviation Research, Washington, DC, Final Report, Feb 2002.

[13] D. Chen, F. Chen, X. Hu., H. Zhang, X. Yin, Y. Zhou. Thermal stability, mechanical and optical properties of novel addition cured PDMS composites with nano-silica sol and MQ silicone resin. *Composites Science and Technology*, *117*, (2015): 307-314,

[14] M. Day, and D. R. Budgell, "Kinetics of thermal degradation of poly(phenylene sulfide)," *Thermochimica Acta*, 203, (1992): 465-474.

[15] J. Ceamanos, J. F. Mastral, A. Millera, and M. E. Aldea, "Kinetics of pyrolysis of high density comparison of isothermal and dynamics experiments," *J. of Analytical and Applied Pyrolysi*s, 65(2), 2002: 93-110.

[16] Cytec technical datasheet of MX2600 chopped molding compound.